Ruthenium(II) Complexes of 2-Aryl-1,10-phenanthrolines: Synthesis, Structure, and Photophysical Properties

Feiyue Wu,[†] Elvira Riesgo,[†] Anna Pavalova,[‡] Rachael A. Kipp,[‡] Russell H. Schmehl,*[,‡] and Randolph P. Thummel*[,†]

Departments of Chemistry, University of Houston, Houston, Texas 7204-56411, and Tulane University, New Orleans, Louisiana 70118

Received June 16, 1999

The synthesis, characterization, and photochemical investigation of a series of Ru(II) complexes having 2-phenyl- and 2,9-diphenyl substituted phenanthroline ligands are reported. Structural characterization of some of the complexes revealed that the phenyl substituents of the phenanthroline ligand are oriented nearly perpendicular to the phenanthroline ring and π-stack with adjacent coordinated 2,2′-bipyridyl ligands. Most of the complexes are nonluminescent at room temperature, and temperature-dependent luminescence studies suggest nonradiative relaxation in solution is dominated by rapid thermally activated internal conversion from the initially populated ^{3}MLCT state to a ligand field (LF) state which decays rapidly to the ground state. The photochemical lability of the complexes was investigated, and it was found that, while the complexes efficiently populate the substitutionally labile LF state, yields for ligand loss are less than expected on the basis of comparison to closely related complexes lacking the phenyl groups which are capable of π-stacking interactions.

Introduction

The ligand 1,10-phenanthroline (phen) has been used to form a wide variety of complexes with Ru(II), and these systems show properties which are remarkably similar to the exhaustively studied complexes of 2,2′-bipyridine (bpy).[1] When a substituent is introduced into the 2- or 9-position of phen, it may interfere somewhat with the complexation process and consequently weaken the ligand field. This results in a large change in the photophysical behavior of the complexes, greatly decreasing the excited-state lifetime and emission quantum yield of the complex in solution at room temperature.[2] However, all complexes of this type reported to date have substituents in the 2- and/or 9-position of the phenanthroline (or the 6- and/or 6′-position of the bipyridine) that are incapable of any interaction with adjacent ligands that would result in stabilization of the complex.

We have recently reported a general method for the preparation of 2-substituted derivatives of phen that takes advantage of the straightforward Friedlander condensation of 8-amino-7-quinolinecarbaldehyde with an enolizable ketone.[3] Aryl ketones such as acetophenone and higher homologues condense smoothly in this fashion and lead to a series of 2-arylphen derivatives. The disposition of the 2-aryl group with respect to the phen depends on the dihedral angle α defined by rotation about the 2,2′-bond. In its extremes, this group can be coplanar ($\alpha = 0°$) or perpendicular ($\alpha = 90°$) with the phen. If one considers a heteroleptic complex of such a ligand L, $[Ru(L)(bpy)_2]^{2+}$, the aryl group will tend toward the perpendicular orientation which will minimize interference with the bpy auxiliary ligands. Such an orientation provides a layered or π-stacked arrangement of the 2-aryl group with an orthogonal bpy and presents the intriguing opportunity for interligand communication (Figure 1).

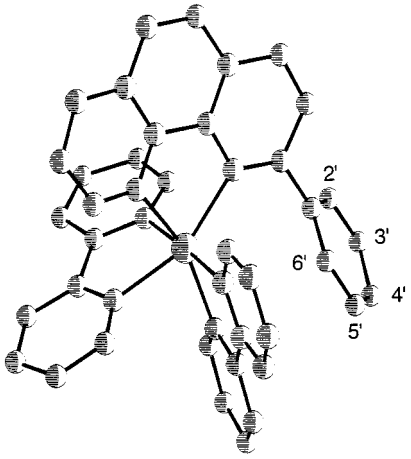

Figure 1. Molecular modeling simulation of $[Ru(bpy\text{-}d_8)_2(\mathbf{3a})]^{2+}$ (PC MODEL).

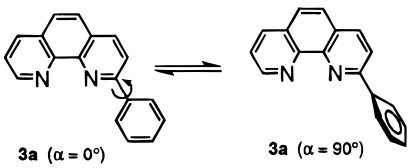

This paper presents the synthesis and spectroscopic investigation of a series of 2-arylphen ligands and their corresponding

[†] University of Houston.
[‡] Tulane University.

(1) (a) Kalyanasundaram, K. *Photochemistry of Polypyridine and Porphyrin Complexes*; Academic Press: San Diego, CA, 1992. (b) Juris, A.; Balzani, V.; Barigelletti, F.; Campagna, S.; Belser, P.; von Zelewsky, A. *Coord. Chem. Rev.* **1988**, *84*, 85.
(2) (a) Fabian, R. H.; Klassen, D. M.; Sonntag, R. W. *Inorg. Chem.* **1980**, *19*, 1977. (b) Kelly, J. M.; Long, C.; O'Connell, C. M.; Vos, J. G.; Tinnemans, A. H. A. *Inorg. Chem.* **1983**, *22*, 2818. (c) Dose, E. V.; Wilson, L. J. *Inorg. Chem.* **1978**, *17*, 2660.
(3) (a) Riesgo, E. C.; Jin, X.; Thummel, R. P. *J. Org. Chem.* **1996**, *61*, 3017. (b) Hung, C.-Y.; Wang, T.-L.; Shi, Z.; Thummel, R. P. *Tetrahedron* **1994,** *50*, 10685.

10.1021/ic990706y CCC: $18.00
Published on Web 11/09/1999

heteroleptic Ru(II) complexes, designed to elucidate possible interligand interactions. The results clearly show that the photophysical behavior of the heteroleptic complexes is similar to other complexes having substituents in the 2- and 9-positions. The photochemistry, however, is more characteristic of complexes having no repulsive interactions between substituents on the diimine ligands. The results are discussed in terms of combined effects of perturbation of the ligand field excited-state energies and stabilization of the excited complex by interligand π-stacking interactions.

Results and Discussion

Synthesis and Characterization. We have previously demonstrated that the Friedländer condensation of 8-amino-7-quinolinecarbaldehyde (**1**) with acetophenone leads to 2-phenyl-

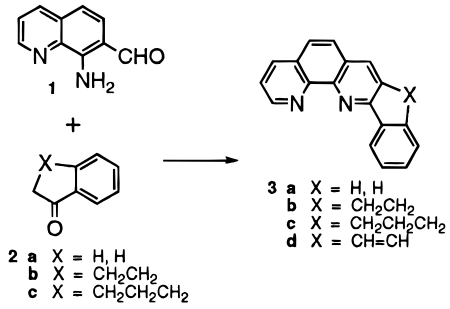

1,10-phenanthroline (**3a**).[2a] When this same reaction is applied to 1-tetralone (**2b**) or benzosuberone (**2c**), the corresponding dimethylene- and trimethylene-bridged derivatives **3b**,**c** can be prepared. Catalytic dehydrogenation of **3b** provides the naphtho-fused phen derivative **3d**.

Two other ligands were prepared for comparison with the series of ligands **3**. The Friedländer condensation of aminoaldehyde **1** with phenylacetaldehyde gave a 21% yield of 3-phenyl-1,10-phenanthroline (**4**), and 2,9-diphenyl-1,10-phenanthroline (**5**) was prepared according to the method of Sauvage and co-workers.[4]

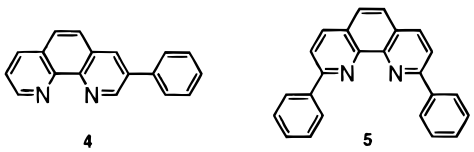

Finally, we chose two ligands which were related to a dimeric form of **3a**: 1,4-bis(2-[1,10]-phenanthrolinyl)benzene (**6**) and

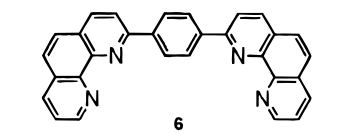

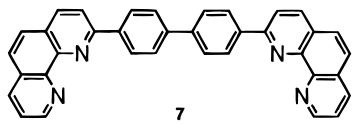

4,4′-bis(2-[1,10]-phenanthrolinyl)biphenyl (**7**). Complexation of these systems with $[Ru(bpy)_2]^{2+}$ will allow the bridging benzene or biphenyl moiety to potentially interact with both metal centers.

Table 1. Dihedral Angle[a] (deg) between the 2-Phenyl Group and the Phen Ring

phen derivative	ligand	$[Ru(bpy\text{-}d_8)_2L]^{2+}$
3a	28.1	54.7
3b	17.2	46.4
3c	34.2	62.6
3d	0	13.8

[a] Calculated using the program PC Model. Dihedral angles are an average of the interior and exterior computed angles.

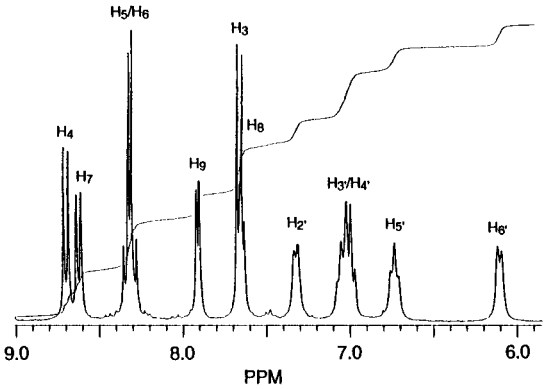

Figure 2. 300 MHz ^{1}H NMR spectrum of $[Ru(bpy\text{-}d_8)_2(\mathbf{3a})](PF_6)_2$ at 25 °C in CD_3CN.

The ligands **3**−**7** were treated with $[Ru(bpy\text{-}d_8)_2Cl_2]$ to afford the mononuclear heteroleptic complexes $[Ru(L)(bpy\text{-}d_8)_2]^{2+}$, where L = **3**−**5**, and the dinuclear heteroleptic complexes $[(bpy\text{-}d_8)_2Ru(L)Ru(bpy\text{-}d_8)_2]^{4+}$, where L = **6** and **7**. The utilization of bpy-d_8 in place of protio-bpy greatly facilitated assignment of the ^{1}H NMR spectra since only signals from the ligands L appeared. In most cases this allowed unambiguous assignments of all signals. The complexes of **3d** and **5** were particularly crowded, and their formation was only possible with the assistance of microwave heating.[5] In these cases the ligand and ruthenium reagent in ethylene glycol were irradiated for 25−30 min to provide 37−46% yields of the desired complexes.

We have carried out energy-minimized molecular mechanics calculations on the ligands **3a**−**d** and their corresponding complexes $[Ru(L)(bpy\text{-}d_8)_2]^{2+}$ with particular attention being paid to the 2,1′-bond which connects the aryl substituent to the phen nucleus (Table 1). For the unbridged parent ligand, 2-phenylphen (**3a**), we calculate a dihedral angle of about 28°, which is consistent with the twist observed in other similar diaryl species. When this ligand is incorporated into the complex $[Ru(\mathbf{3a})(bpy\text{-}d_8)_2]^{2+}$, the dihedral angle almost doubles to an estimated 55°, and from Figure 1 we can see that this twisted conformation is stabilized by apparent π-stacking between the 2-phenyl ring and one pyridine of an auxiliary bpy-d_8. Analysis of the ^{1}H NMR of this complex shows temperature-dependent behavior of the 2-phenyl ring (Figure 2). At room-temperature we observe five signals for this ring, shifted upfield due to shielding from the π-stacking effect. The two *ortho*-protons (H2′ and H6′) appear as doublets differentiated by about 1.2 ppm with the higher field doublet being assigned to H6′, which is held over the more central region of the auxiliary bpy-d_8. All five protons are slightly broadened at room temperature indicat-

(4) Dietrich-Buchecker, C. O.; Marnot, P. A.; Sauvage, J. P. *Tetrahedron Lett.* **1982**, *23*, 5291.

(5) (a) Matsumura-Inoue, T.; Tanabe, M.; Minami, T.; Ohashi, T. *Chem. Lett.* **1994**, 2443. (b) Arai, T.; Matsumura, T.; Oka, T. *Kagaku to Kyouiku* **1993**, *41*, 278 (Chemistry and Education, Japanese).

Table 2. ^{1}H NMR Chemical Shift Data[a] for 2-Phenyl Substituent in Ru(II) Complexes

complex	H2′	H3′	H4′	H5′	H6′
[Ru(**3a**)(bpy-d_8)$_2$]$^{2+}$	7.32	7.05	7.00	6.73	6.10
[Ru(**3b**)(bpy-d_8)$_2$]$^{2+}$ [b]		7.01	6.94	6.80	7.69
[Ru(**3c**)(bpy-d_8)$_2$]$^{2+}$		*c*	*c*	6.47	5.46
[Ru(**3d**)(bpy-d_8)$_2$]$^{2+}$		9.14	7.16	7.41	7.73
[Ru(**4**)(bpy-d_8)$_2$]$^{2+}$	7.56	7.48	7.48	7.48	7.56
[Ru(**5**)(bpy-d_8)$_2$]$^{2+}$	7.12	6.85	7.01	6.72	6.11
[(bpy-d_8)$_2$Ru(**6**)Ru(bpy-d_8)$_2$]$^{4+}$	6.79 (d)	5.89 (d)		6.79 (d)	5.89 (d)
	7.11 (s)	7.11 (s)		5.32 (s)	5.32 (s)
[(bpy-d_8)$_2$Ru(**7**)Ru(bpy-d_8)$_2$]$^{4+}$	7.40	7.12		6.79	6.22

[a] Measured at room temperature and reported in ppm referenced to CH_3CN at 1.93 ppm. [b] Measured at −40 °C. [c] Overlapping peaks, difficult to assign; clear evidence for more than four signals implying two conformers.

Table 3. ^{1}H NMR Chemical Shift Data[a] for Phenanthroline Protons in Ru(II) Complexes

complex	H2	H3	H4	H5/H6	H7	H8	H9
[Ru(phen)(bpy-d_8)$_2$]$^{2+}$	8.07	7.72	8.60	8.23	8.60	7.72	8.07
[Ru(**3a**)(bpy-d_8)$_2$]$^{2+}$		7.66	8.69	8.31	8.62	7.65	7.90
[Ru(**3b**)(bpy-d_8)$_2$]$^{2+}$ [b]			8.33	8.16	8.61	7.56	7.83
[Ru(**3c**)(bpy-d_8)$_2$]$^{2+}$			8.42	8.22	8.57	7.64	8.06
			8.55	8.25	8.61	7.59	7.84
[Ru(**3d**)(bpy-d_8)$_2$]$^{2+}$			8.96	8.24	8.69	7.68	7.94
[Ru(**4**)(bpy-d_8)$_2$]$^{2+}$	8.15		8.83	8.26	8.62	7.73	8.08
[Ru(**5**)(bpy-d_8)$_2$]$^{2+}$		7.53	8.65	8.33	8.65	7.53	
[Ru$_2$(**6**)(bpy-d_8)$_4$]$^{4+}$ [c]		7.38	8.81	8.33	8.63	7.65	7.89
		7.42	8.83	8.34	8.61	7.66	7.87
[Ru$_2$(**7**)(bpy-d_8)$_4$]$^{4+}$		7.72	8.75	8.34	8.64	7.66	7.90

[a] Measured in CD_3CN at 300 MHz and 25 °C and reported in ppm referenced to CH_3CN at 1.93 ppm. [b] Measured at −40 °C.

ing some restricted movement of the ring in the complex. As the temperature is raised, the pairs of protons H2′, H6′ and H3′, H5′ begin to coalesce, a process which is complete at about 65 °C where the phenyl ring is now freely rotating on the NMR time scale. The H4′ proton remains unaffected. From this VT experiment a rotational barrier of 16.3 kcal/mol can be estimated.

When the 3-phenylphen system [Ru(**4**)(bpy-d_8)$_2$]$^{2+}$ is considered for comparison, one observes H2′ and H6′ as a two proton doublet at 7.56 ppm and the remaining three protons show two overlapping signals at 7.48 ppm. The equivalence of H2′ and H6′ as well as H3′ and H5′ indicates free rotation about the phenylphen bond while the lower field resonance of these protons indicates a lack of shielding due to any π-stacking.

For the dimethylene-bridged system, **3b**, a smaller dihedral angle of about 17° is enforced for the free ligand and rapid inversion of the bridge is occurring on the NMR time scale. In the mixed-ligand complex of **3b**, steric crowding of the phenyl ring increases the dihedral angle to an estimated 46° at the apparent expense of substantial strain in the bridge. The phenyl ring can now be twisted in two distinctly different conformations with respect to the other bpy-d_8 ligands around the metal. If these conformations were noninterconverting, we would expect to see two sets of signals for the phenyl ring protons. However, only one well-dispersed set of signals is observed, indicating that, at room temperature on the NMR time scale, the phenyl ring is flipping rapidly back and forth through inversion of the dimethylene bridge.

Calculations indicate that **3c** should be more similar to the unbridged ligand **3a** with a large twist angle for the 2′-phenyl ring. In the mixed-ligand complex twisting about the 2,2′-bond is slow on the NMR time scale and thus we observe two distinct diastereomeric conformations. The phenyl protons are again highly shielded, and clear single proton signals at 5.46 and 6.47 ppm each integrate for less than one H, consistent with the complex being a mixture of diastereomers.

The 2,9-diphenylphen system **5** should rather closely resemble **3a**; the main difference in the mixed-ligand complex is that now each phenyl ring overlaps with a different bpy-d_8, the system has higher symmetry, and all the ligands are potentially interacting. The complex [Ru(**5**)(bpy-d_8)$_2$]$^{2+}$ shows five distinct phenyl signals at room temperature. Four of them are broad singlets while H4′, which does not change its relative orientation with rotation about the 2,1′-bond, appears as a sharp triplet at 7.01 ppm. The signals are assigned by analogy to the complex of **3b** with H2′ and H3′ being shifted 0.20 ppm to higher field.

Table 3 summarizes the chemical shift data for the phenanthroline protons in the complexes. These are all fairly well behaved, and one can observe reasonable consistency through the table. The proton H9, that is the most downfield in the free ligands, is shifted upfield due to shielding by one of the orthogonal bpy-d_8 ligands. This effect is amplified along the series phen, **3a**, and **3b** as the effective bulk of the 2-substituent forces H9 closer to the orthogonal ligand.

The dinuclear complexes show unique behavior because now the 2-phenyl substituent serves as a link between two similar [Ru(bpy-d_8)]$^{2+}$ units. In [(bpy-d_8)$_2$Ru(**6**)Ru(bpy-d_8)$_2$]$^{4+}$ the bridging benzene ring is layered between a bpy-d_8 on each of the metals, forming a double-decked π-sandwich. The absolute configuration (Δ or Λ) at each of the metal centers now plays a role in determining the symmetry of the system. When both metals have the same configuration (Δ,Δ or Λ,Λ), then the protons H2 and H3 as well as H5 and H6 on the bridging benzene are equivalent, do not split each other, and give rise to a singlet. However, when the metals have opposite configurations (Δ,Λ or Λ,Δ), then H2 is identical to H5 but different from H3, which is identical to H6. In this case these adjacent nonequivalent protons split one another into a doublet. Being in the middle of the "π-stacked sandwich", these benzene protons are shifted considerably upfield and are clearly evident and diagnostic of configuration. Figure 3 shows the downfield region of the ^{1}H NMR for this complex where the Δ,Δ or Λ,Λ complex exhibits singlets at 7.11 and 5.32 ppm for H2/H3 and H5/H6, respectively, while the Δ,Λ or Λ,Δ complex shows doublets at 6.79 and 5.89 ppm for H2/H5 and H3/H6, respec-

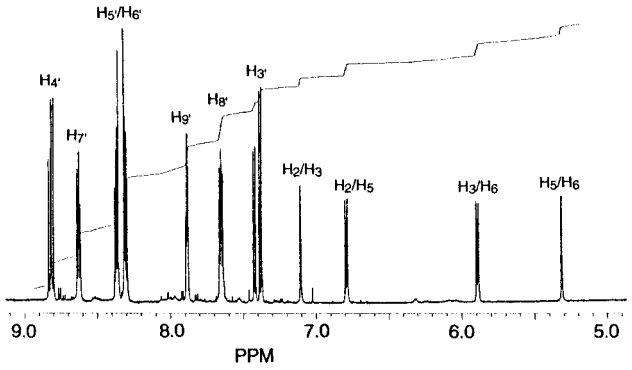

Figure 3. 600 MHz ^{1}H NMR spectrum of [(bpy-d_8)$_2$Ru(**6**)Ru(bpy-d_8)$_2$](PF$_6$)$_4$ at 25 °C in CD_3CN.

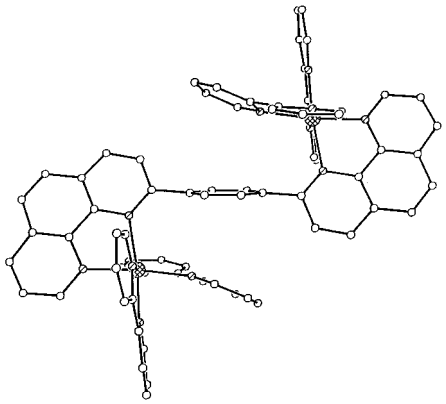

Figure 4. Side view of [(bpy)$_2$Ru(**6**)Ru(bpy)$_2$]$^{4+}$.

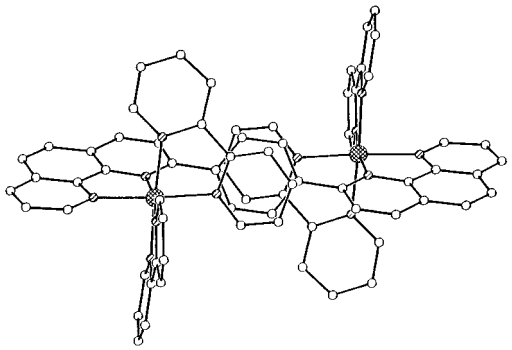

Figure 5. Top view of [(bpy)$_2$Ru(**6**)Ru(bpy)$_2$]$^{4+}$.

tively. Integration of these peaks indicates about a 3:2 ratio of the Δ,Λ or Λ,Δ to the Δ,Δ or Λ,Λ complex. It is noteworthy that all the phenanthroline resonances are also well resolved and each one is "twinned" in the same 3:2 ratio but the chemical shift differences between these sets of peaks are much smaller.

To further investigate the π-sandwich behavior of this complex, we carried out a single-crystal X-ray analysis on its perprotio analogue, and a top and side view of the cation are given in Figures 4 and 5. Each "half" of the molecule resembles the corresponding mononuclear complex [Ru(**3a**)(bpy-d_8)$_2$]$^{2+}$ as pictured in Figure 1. One pyridine of an auxiliary bpy on each metal forms the outer layer of the π-stack and is consequently twisted out of coplanarity with its attached pyridine. This twist angle is 21.6° while the other auxiliary bpy remains more planar with a dihedral twist of only 7.5°. As expected, the phen portion of the molecule is quite planar with its two pyridine halves twisting only 3.2° out of coplanarity. The bridging benzene and its two appended phens are not quite orthogonal, making an angle of 60.5° which helps to alleviate some of the steric repulsion between the layers in the π-stack.

The three rings comprising the central π-stack are not arranged in exactly parallel planes. If one considers the best mean plane through each of these rings, the outer pyridine and central benzene describe a dihedral angle of about 24.5°. The distance of any atom in one ring to the mean plane described by the adjacent ring varies from 2.91 to 4.21 Å, affording an average of 3.56 Å which is essentially the van der Waals distance between two parallel aromatic rings.

The Ru−N bond lengths also reflect the distortion caused by crowding in the center of the molecule. Of the six Ru−N bonds, five of them fall in the range of 2.05−2.08 Å, while the bond to the nitrogen of the π-stacked pyridine is lengthened to 2.13 Å.

The dinuclear complex [(bpy-d_8)$_2$Ru(**7**)Ru(bpy-d_8)$_2$]$^{4+}$ truly represents a dimer of [Ru(**3a**)(bpy-d_8)$_2$]$^{2+}$ joined at the 4′-position of the phenyl ring. We would expect the structure to be a benzalogue of the dinuclear complex of **6** with the main difference being flexibility about the central bond between the two halves of the bridging biphenyl. This flexibility essentially disrupts any communication between the two metal centers. As for [Ru(**3a**)(bpy-d_8)$_2$]$^{2+}$, the phenyl ring protons are all nonequivalent so that a spectrum very similar to Figure 2 is obtained, lacking the 4′-proton resonance. Like the complex of **6**, the dinuclear complex of **7** should exist as a pair of diastereomers formed in roughly equal amounts. In this case, however, we do not observe twinning of the NMR peaks since the two metal centers are sufficiently separate that they do not influence one another. The biphenyl protons do show some broadening at room temperature due to rotation about the central bond.

The half-wave redox potentials for the ruthenium complexes were measured by cyclic voltammetry in acetonitrile, and the results are collected in Table 4. All the complexes show an oxidation wave in the range of +1.30−1.35 V, indicating that removal of a d-orbital electron on ruthenium requires approximately the same energy regardless of the disposition of a 2′-substituent on phenanthroline. The reduction potentials also fall within a narrow range and resemble the unsubstituted phen complex, −1.25 to −1.30 V for the first reduction and −1.48 to −1.55 V for the second reduction. Most of the waves appear to be clearly reversible or quasi-reversible.

Photochemical and Photophysical Behavior. Room-temperature absorption and luminescence properties of all the complexes are given in Table 5. The entire set of complexes, both monometallic and bimetallic, have absorption maxima for the Ru(II) dπ → (diimine) π* metal-to-ligand charge transfer (MLCT) transitions between 440 and 450 nm in CH_3CN solution. Room-temperature luminescence is observed from all the monometallic complexes except for the complex of ligand **3d**, and maxima are between 610 and 625 nm. The two bimetallic complexes are nonluminescent at room temperature. The parent complex of the series, [Ru(phen)(bpy-d_8)$_2$]$^{2+}$, has an emission maximum of 615 nm, an emission quantum yield of 0.06, and a luminescence lifetime of 760 ns in N_2-degassed CH_3CN. The values are similar to those measured by Caspar and Meyer for the same complex in CH_2Cl_2.[6] All of the complexes having a phenyl substituent in the 2- or 2- and 9-positions of the phenanthroline (**3a**−**d**, **5**−**7**) are at best only very weakly luminescent at room temperature, with measured quantum yields less than 0.001. Luminescence lifetimes for these complexes are also very short (<5 ns); the results indicate that

(6) Caspar, J. V.; Meyer, T. J. *Inorg. Chem.* **1983**, *22*, 2444.

Table 4. Half-Wave Redox Potentials for Ruthenium Complexes

complex	$E_{1/2}$, ox	$E_{1/2}$, red		
$[Ru(phen)(bpy\text{-}d_8)_2]^{2+}$	+1.32 (82)	−1.30 (91)	−1.49 (112)	
$[Ru(\mathbf{3a})(bpy\text{-}d_8)_2]^{2+}$	+1.32 (66)	−1.28 (71)	−1.50 (72)	−1.83 (81)
$[Ru(\mathbf{3b})(bpy\text{-}d_8)_2]^{2+}$	+1.30 (71)	−1.30 (71)	−1.51 (91)	−1.78 (91)
$[Ru(\mathbf{3c})(bpy\text{-}d_8)_2]^{2+}$	+1.32 (82)	−1.30 (81)	−1.55 (102)	−1.84 (101)
$[Ru(\mathbf{3d})(bpy\text{-}d_8)_2]^{2+}$	+1.34 (71)	−1.45 (70)	−1.72 (92)	
$[Ru(\mathbf{4})(bpy\text{-}d_8)_2]^{2+}$	+1.33 (71)	−1.26 (71)	−1.48 (82)	−1.72 (92)
$[Ru(\mathbf{5})(bpy\text{-}d_8)_2]^{2+}$	+1.32 (82)	−1.25 (101)	−1.55 (153)	
$[(bpy\text{-}d_8)_2Ru(\mathbf{6})Ru(bpy\text{-}d_8)_2]^{4+}$	+1.35 (127)			
$[(bpy\text{-}d_8)_2Ru(\mathbf{7})Ru(bpy\text{-}d_8)_2]^{4+}$	+1.34 (51)			

[a] Potentials are in volts vs SCE, and most waves were reversible. The mV difference between the anodic and cathodic wave is given in parentheses.

Table 5. Photophysical Properties of Ruthenium Complexes

		emission (298 K)[a]			
complex	abs: λ_{max} (log ϵ)	λ_{max}(nm)	ϕ_{em}	τ_{em}(ns)	photoanation[b] ϕ_p
$[Ru(phen)(bpy)_2]^{2+}$	448 (4.31)	615	0.06	760	0.52
$[Ru(\mathbf{3a})(bpy)_2]^{2+}$	447 (4.28)	622	0.0007	5	0.56
$[Ru(\mathbf{3b})(bpy)_2]^{2+}$	447 (4.18)	618	0.0003	3	0.59
$[Ru(\mathbf{3c})(bpy)_2]^{2+}$	444 (4.17)	624	0.0004	<1	0.25
$[Ru(\mathbf{3d})(bpy)_2]^{2+}$	444 (4.06)				0.79
$[Ru(\mathbf{4})(bpy)_2]^{2+}$	450 (4.18)	610	0.09	698	0.69
$[Ru(\mathbf{5})(bpy)_2]^{2+}$	445 (4.04)	619	0.0006	<1	0.3
$[Ru(bpy)_2(\mathbf{6})Ru(bpy)_2]^{4+}$	447 (4.41)	NA	NA	NA	0.07
$[Ru(bpy)_2(\mathbf{7})Ru(bpy)_2]^{4+}$	448 (4.39)	NA	NA	NA	0.11

[a] In N_2-purged CH_3CN. NA = not measurable. [b] Yields for Cl^- photoanation in CH_3Cl relative to $[Ru(bpy)_3]^{2+}$.

Table 6. Luminescence Properties of Ruthenium Complexes

	emission (77 K)		activatn params excited state decay				
complex	E_{00} (cm^{-1})[a]	τ_{em} (μs)	k_0 (s^{-1})	E_a (cm^{-1})	k' (s^{-1})	η_{LF}	ϕ_{rel}[c]
$[Ru(bpy)_2(phen)]^{2+}$	17 525	7.1	7×10^5	2576	3×10^{11}	0.63	1.0
$[Ru(\mathbf{3a})(bpy)_2]^{2+}$	17 300	5.7	2×10^5	1660	7×10^{11}	1.00	0.7
$[Ru(\mathbf{3b})(bpy)_2]^{2+}$[b]	16 950	7.1	3×10^6	1160	2×10^{11}	1.00	0.7
$[Ru(\mathbf{3c})(bpy)_2]^{2+}$	17 220	6.7	1×10^6	1540	6×10^{11}	1.00	0.3
$[Ru(\mathbf{3d})(bpy)_2]^{2+}$	15 100	4.6	3×10^5	2600	4×10^{11}	0.82	1.2
$[Ru(\mathbf{4})(bpy)_2]^{2+}$	17 400	8.0	2.2×10^5	2790	1×10^{12}	0.86	1.0
$[Ru(\mathbf{5})(bpy)_2]^{2+}$	17 180	9.3	1.1×10^5	1190	9×10^{11}	1.00	0.4
$[Ru(bpy)_2(\mathbf{6})Ru(bpy)_2]^{4+}$	17 200	6.1	3×10^5	1520	3×10^{11}	1.00	0.1
$[Ru(bpy)_2(\mathbf{7})Ru(bpy)_2]^{4+}$	17 210	6.8	3×10^5	1721	6×10^{11}	1.00	0.1

[a] Obtained from fits of 77 K emission spectrum to eq 1. [b] Lowest temperature used in fit = 130 K. [c] Substitution quantum yield divided by η_{LF} and normalized to the value for the phen complex.

the difference in behavior relative to $[Ru(phen)(bpy\text{-}d_8)_2]^{2+}$ is due to changes in the rate constant for nonradiative relaxation of the complexes (vide infra).[7] The complex of **4**, having a phenyl in the 3-position, has absorption and emission maxima very similar to those of the phen complex. In addition, the complex exhibits strong luminescence and has a larger emission quantum yield than the phen complex.

The bimetallic complexes of ligands **6** and **7** have absorption maxima for the MLCT transition that are nearly the same as the monometallic complexes. The complexes are nonluminescent in room-temperature solution. From the redox and spectrophotometric behavior it is clear that the electronic interaction between the two metal centers is small. Recent studies of exchange energy transfer in bimetallic complexes having two bipyridyl ligands linked by a phenyl bridge in the 4-position of the bipyridine also were relatively weakly coupled; the electronic coupling matrix element for the energy transfer was estimated to be approximately 50 cm^{-1}.[8]

All the complexes exhibit strong luminescence in ethanol/methanol glasses at 77 K. Table 6 lists luminescence lifetimes of the complexes in the glass and E_{00} energies obtained from fits of emission spectra obtained at 77 K. Figure 6 shows 77 K emission spectra of $[Ru(phen)(bpy\text{-}d_8)_2](PF_6)_2$ and $[Ru(\mathbf{3d})(bpy\text{-}d_8)_2](PF_6)_2$ and fits of the spectra employing a single mode Franck−Condon analysis, initially used by Meyer and coworkers and subsequently used by others.[8−10] The approach calculates the normalized luminescence intensity, I_v, as a function of frequency assuming averaged medium- and low-frequency vibrational modes, $h\omega_m$ and $h\omega_l$, and the corresponding electron−vibrational coupling constants, S_m and S_l (eq 1). Broadening of the individual vibronic components is included in eq 1 as the half-widths, ν_h.

$$I_\nu = \sum_m \sum_l \left[\left(\frac{E_0 - mh\omega_m - lh\omega_l}{E_0}\right)^3\right] \frac{S_m^m}{m!} \frac{S_l^l}{l!} \exp\left[-4\ln 2\left(\frac{\nu - E_0 + mh\omega_m + lh\omega_l}{\nu_h}\right)^2\right] \quad (1)$$

In the fits $h\nu_l$ and S_l were fixed at 465 cm^{-1} and 0.8, respectively and E_o, $h\nu_m$, S_m, and ν_h were varied. Best fit values for $h\nu_m$ ranged from 1300 (for $[Ru(\mathbf{3d})(bpy\text{-}d_8)_2]^{2+}$) to 1400 cm^{-1}; values for S_m were between 0.49 (for $[Ru(\mathbf{3d})(bpy\text{-}d_8)_2]^{2+}$) and 0.79 (for $[(bpy\text{-}d_8)_2Ru(\mathbf{6})Ru(bpy\text{-}d_8)_2]^{4+}$), and ν_h values ranged from 650 to 1100 cm^{-1}. Values obtained are thus typical

(7) (a) Meyer, T. J. *Pure Appl. Chem.* **1986**, *58*, 1193. (b) Caspar, J. V.; Meyer, T. J. *J. Phys. Chem.* **1983**, *87*, 952.
(8) Liang, Y.; Baba, A. I.; Schmehl, R. H. *J. Phys. Chem.* **1996**, *100*, 18408.

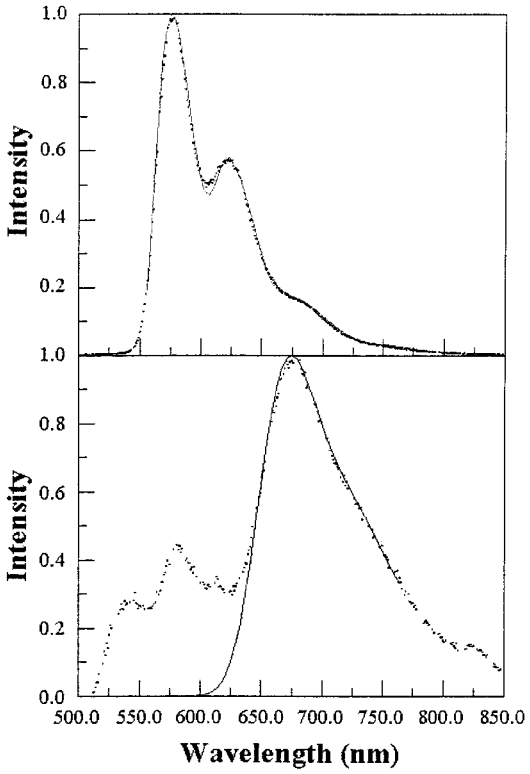

Figure 6. Emission spectra of $[Ru(phen)(bpy)_2](PF_6)_2$ (top) and $[Ru(\mathbf{3d})(bpy)_2](PF_6)_2$ in 4:1 EtOH/MeOH at 77 K. The solid lines represent fits to the data using eq 1 and parameters given in the text and Table 6.

of values obtained for Ru(II) diimine complexes in frozen matrixes.[8−10]

The low-temperature luminescence spectra clearly illustrate that most of the complexes have emission maxima and decays that do not differ significantly from the parent complex, $[Ru(phen)(bpy\text{-}d_8)_2]^{2+}$. All the monometallic and bimetallic complexes having phenyl substituents in the 2- or 3-position of the phenanthroline ligand have E_0 values within 300 cm^{-1} of 17 200 cm^{-1} and lifetimes within 20% of that of the parent phenanthroline complex. Thus, the steric and electronic perturbations introduced by phenyl substitution in the 2-position of the phenanthroline result in only very slight changes in the spectroscopic parameters. The significant exception is $[Ru(\mathbf{3d})(bpy\text{-}d_8)_2]^{2+}$, which has an E_0 of 15 100 cm^{-1} and a lifetime at 77 K of 4.6 μs. This naphtho-fused phenanthroline derivative is the only ligand with extended unsaturation. The much lower energy luminescence maximum is similar to that of Ru(II) pyridylquinoline complexes ($[Ru(pq)(bpy)_2]^{2+}$, where pq = 2-(2′-pyridyl)quinoline, has a maximum of 14 900 cm^{-1} at 77 K).[11]

Substantial differences were observed, however, in the temperature dependence of the luminescence decays. Figure 7 illustrates the range of behavior observed in luminescence decay rate constants ($1/\tau_{em}$) as a function of temperature for three of

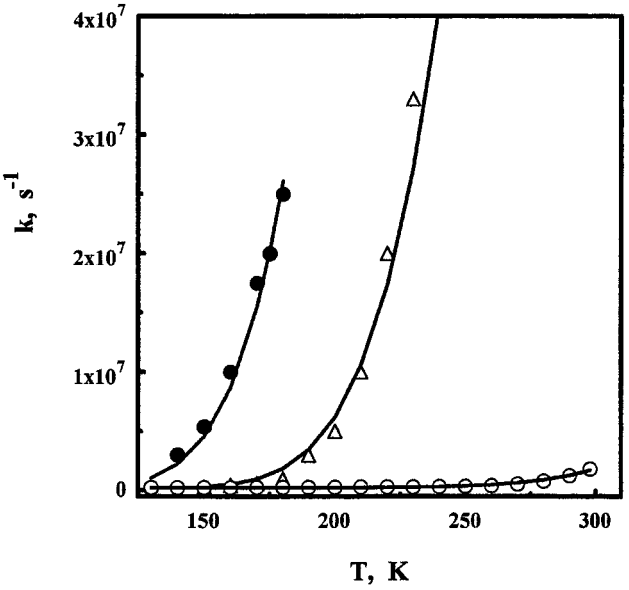

Figure 7. Temperature dependence of luminescence decay rate constants for $[Ru(\mathbf{3a})(bpy)_2](PF_6)_2$ (open triangles), $[Ru(\mathbf{3b})(bpy)_2](PF_6)_2$ (filled circles), and $[Ru(phen)(bpy)_2](PF_6)_2$ (open circles). Solid lines represent fits to the data using eq 2; parameters for the fits are given in Table 6.

the complexes. The temperature dependence of each was fit by assuming a model wherein the MLCT state relaxes through two channels: a temperature-independent relaxation associated with radiative and nonradiative decay from the MLCT state (k_0) and a thermally activated decay to another state which decays rapidly to the ground state. The thermally activated crossover from the MLCT state to the rapidly decaying state has an activation energy, E_a, and a prefactor, k'. This approach has been used extensively in fitting temperature-dependent luminescence decay data.[12−17] Data were fit to eq 2 using a least-squares fitting

$$1/\tau = k = k_o + k' \exp(-E_a/RT) \qquad (2)$$

routine, and parameters for the fits are given in Table 6. Investigation of related Ru(II) diimine complexes has yielded very similar temperature-dependent luminescence behavior. For example, $[Ru(bpy)_2(py)_2]^{2+}$ (py = pyridine) is nonluminescent at room temperature but becomes strongly luminescent below 200 K; the temperature dependence of the luminescence has been fit to eq 2 and yields values for k′ and E_a of 2.3×10^{14} s^{-1} and 2758 cm^{-1}, respectively.[16a] The complex loses pyridine upon photolysis at room temperature, and the temperature dependence of the light induced ligand loss mirrors the temperature dependence of the luminescence. The rapidly decaying state populated by thermally activated crossover from the MLCT state in this and other related complexes was

(9) (a) Barqawi, K. R.; Murtaza, Z.; Meyer, T. J. *J. Phys. Chem.* **1991**, *95*, 47. (b) Kober, E. M.; Caspar, J. V.; Lumpkin, R. S.; Meyer, T. J. *J. Phys. Chem.* **1986**, *90*, 3722. (c) Caspar, J. V.; Westmoreland, T. D.; Allen, G. H.; Bradley, P. G.; Meyer, T. J.; Woodruff, W. H. *J. Am. Chem. Soc.* **1984**, *106*, 3492.
(10) Rillema, D. P.; Blanton, C. B.; Shaver, R. J.; Jackman, D. C.; Boldaji, M.; Bundy, S.; Worl, L.; Meyer, T. J. *Inorg. Chem.* **1992**, *31*, 1600. (b) Blanton, C. B.; Murtaza, Z.; Shaver, R. J.; Rillema, D. P. *Inorg. Chem.* **1992**, *31*, 3230.
(11) Klassen, D. M. *Chem. Phys. Lett.* **1982**, *93*, 383.
(12) Van Houten, J.; Watts, R. J. *J. Am. Chem. Soc.* **1976**, *98*, 4853.
(13) (a) Hipps, K. W.; Crosby, G. A. *J. Am. Chem. Soc.* **1975**, *97*, 7042. (b) Hager, G. D.; Watts, R. J.; Crosby, G. A. *J. Am. Chem. Soc.* **1975**, *97*, 7037.
(14) Caspar, J. V.; Nagle, J. K.; Meyer, T. J. *J. Am. Chem. Soc.* **1982**, *104*, 4803.
(15) Macatangay, A.; Zheng, G. Y.; Rillema, D. P.; Jackman, D. C.; Merkert, J. W. *Inorg. Chem.* **1996**, *35*, 6823.
(16) (a) Wacholtz, W. F.; Auerbach, R. A.; Schmehl, R. H.; Ollino, M.; Cherry, W. R. *Inorg. Chem.* **1985**, *24*, 1758. (b) Wacholtz, W. F.; Auerbach, R. A.; Schmehl, R. H. *Inorg. Chem.* **1986**, *25*, 227.
(17) (a) Barigelletti, F.; Belser, P.; von Zelewsky, A.; Juris, A.; Balzani, V. *J. Phys. Chem.* **1985**, *89*, 3680−4. (b) Barigelletti, F.; Juris, A.; Balzani, V.; Belser, P.; von Zelewsky, A. *J. Phys. Chem.* **1986**, *90*, 5190.

postulated to be a triplet ligand field excited state of the metal. The temperature dependence of the MLCT excited-state decay of $[Ru(bpy)_3]^{2+}$ and numerous other Ru(II) diimine complexes has also been attributed to activated population of a ligand field (LF) excited state.[12−17]

Some Ru(II) diimine complexes exhibit only weakly temperature dependent excited-state relaxation rate constants. While data for these complexes can usually be fit using an expression identical to eq 2, the interpretation of the thermally activated process differs.[7a] This group of complexes has much lower k' values (typically $< 10^{10}$ s^{-1}), and activation barriers are generally considerably less than 1000 cm^{-1}. The thermally activated process for these systems has been attributed to population of another MLCT state having significant singlet character.

Of the complexes examined in this work, all the complexes with phenyl moieties in the 2-position (**3a**−**c**, **5**−**7**) exhibit strong temperature dependence and have activation barriers between 1100 and 1800 cm^{-1}. The complex with 2,9-diphenylphen, $[Ru(\mathbf{5})(bpy)_2]^{2+}$, is essentially nonluminescent at temperatures above 160 K while the complex with a single 2-phenyl substituent, $[Ru(\mathbf{3a})(bpy\text{-}d_8)_2]^{2+}$, exhibits reasonably intense emission up to approximately 250 K. Both complexes have activation parameters that resemble complexes for which population of a ligand field state is postulated.

The phenyl substituent in $[Ru(\mathbf{3a})(bpy\text{-}d_8)_2]^{2+}$ is free to rotate, allowing optimal π-stacking with an auxiliary bipyridine. Ligands **3b**,**c** have di- and trimethylene bridges, respectively, tethering the 2-phenyl substituent and the phenanthroline. In the complex of **3b**, the phenyl is held more coplanar with the phenanthroline and π-stacking interactions are less likely. As a result, this complex has a significantly lower activation energy for crossover to the LF state and is nonluminescent at temperatures above approximately 180 K. The torsion angle between the phenanthroline and its phenyl substituent is larger for the complex of **3c** than for **3b**, and the temperature dependence of the luminescence decay is much more like that of the complex of **3a**, having an untethered phenyl. The observed temperature-dependent luminescence suggests that introduction of phenyl moieties in the 2- (and 2,9-) position(s) results in an overall lowering of the energy of the LF excited states since the activation barrier for populating the LF state is lowered significantly relative to the parent complex ($[Ru(phen)(bpy)_2]^{2+}$). However, the ability of the 2-phenyl group to π-stack with adjacent bipyridine ligands does serve to stabilize the LF state of these complexes relative to the complex having a sterically constrained 2-phenyl substituent that is unable to π-stack.

The temperature-dependent luminescence decay data indicate that the loss of room-temperature luminescence from the complexes having phenyl (or tethered phenyl) substituents in the 2- (or 2,9-) position(s) is a result of weakening the ligand field of the complex. The weakened ligand field allows facile crossover from the ^{3}MLCT state manifold to a ^{3}LF state. The temperature-dependent luminescence decay data allows estimation of the efficiency of populating the ^{3}LF state, η_{LF}, using eq 3.

$$\eta_{LF} = [k' \exp(-E_a/RT)]/[k_0 + k' \exp(-E_a/RT)] \qquad (3)$$

Efficiencies at 298 K are given in Table 6. The results show that all the complexes, including the phen complex, efficiently internally convert to the ^{3}LF state, but the complexes having 2-phenyl substituents on the phen cross to the ^{3}LF state with 100% efficiency. The implication is that the complexes of **3a**−**7** (with the exception of **3d** and **4**) should be more substitutionally labile, since the ligand field state is known to be much more labile than the MLCT state. However, the measured quantum yields reported in Table 5 show little variation among the complexes. In fact, the bimetallic complexes have intersystem crossing efficiencies approaching unity yet have the lowest photoanation yields.

The quantum yield for photosubstitution can be represented as the product of three terms (eq 4): (1) the efficiency of

$$\phi_p = \eta_{MLCT}\eta_{LF}\eta_{product} \qquad (4)$$

forming the ^{3}MLCT state from the initially populated ^{1}MLCT state; (2) the efficiency of internal conversion to the ^{3}LF state (eq 3), (3) the ligand substitution efficiency of the ^{3}LF state. Yields for population of the ^{3}MLCT state have been measured for several Ru(II) diimine complexes and are generally close to unity.[16b,18] By assuming $\eta_{MLCT} = 1$ and using the measured values for η_{LF} and the experimental quantum yields for photoanation with Cl^- in $CHCl_3$ from Table 5, the relative efficiency for substitution of the ^{3}LF state, η_{rel} ($\phi_{p,complex}\eta_{LF,phen}/\eta_{LF,complex}\phi_{p,phen}$) can be determined. Table 6 lists η_{rel} values normalized relative to the value for the phen complex. All of the complexes having 2-phenyl substituents are *less* labile than the other complexes, including the complex having a 3-phenyl substituent. Among the monometallic complexes, the complex with 2,9-diphenylphen (**5**) has a lower relative substitution yield than the complexes with free or tethered phenyl substituents in only the 2-position of the phenanthroline. In addition, the complex with the dimethylene-bridged 2-phenylphen (**3b**) has the highest relative substitutional reactivity of the 2-phenyl-substituted derivatives. The explanation for the low photoreactivity of the bimetallic complexes of **6** and **7** may be related to the fact that multiple π-stacking interactions exist. We are presently examining this possibility in greater detail.

Conclusions

The synthesis, structural characterization, and spectroscopic investigation of Ru(II) diimine complexes having interligand π-stacking interactions are presented. The crystallographic data clearly illustrate that the average distance between a 2-aryl substituent on a phenanthroline ligand and the π-stacked pyridine of an adjacent bipyridine ligand is essentially the van der Waals separation; thus significant π-interactions between neighboring ligands are possible. The photophysical behavior of the complexes is dominated by rapid population of the ^{3}LF excited states that are known to be substitutionally labile. The combined photophysical and photochemical evidence argues for stabilization of the labile LF excited state of the complexes, and this stabilization is believed to be due to the interligand π-stacking interactions.

Experimental Section

Nuclear Magnetic Resonance spectra were recorded on a General Electric QE-300 spectrometer at 300 MHz for ^{1}H and 75 Mz for ^{13}C or a Bruker AMX-600 spectrometer at 600 MHz for ^{1}H. UV spectra were obtained on a Perkin-Elmer Lambda 3B spectrophotometer. Fluorescence spectra were obtained on either a Perkin-Elmer LS 50 Luminescence spectrometer or a SPEX 111 spectrofluorometer. Luminescence lifetimes at room temperature and variable-temperature lifetimes were obtained using equipment and methods described elsewhere.[13] Mass spectra were obtained on a Hewlett-Packard 5989B mass spectrometer (59987A electrospray) using atmospheric pressure

(18) (a) Bolletta, F.; Juris, A.; Maestri, M.; Sandrini, D. *Inorg. Chim. Acta* **1980**, *44*, 6175. (b) Bensasson, R.; Salet, C.; Balzani, V. *J. Am. Chem. Soc.* **1976**, *98*, 3722.

ionization at 160 °C. Cyclic voltammograms were recorded using a BAS CV-27 voltammograph and a Houston Instruments model 100 X-Y recorder according to a procedure which has been described previously.[14] A household microwave oven (Samsung, model MW 2000 U) was modified according to a previously published description.[5b] Elemental analyses were performed by National Chemical Consulting, P.O. Box 99, Tenafly, NJ 07670.

8-Amino-7-quinolinecarbaldehyde,[3a] 2,9-diphenyl-1,10-phenanthroline,[4] and *cis*-[Ru(bpy-d_8)$_2$Cl$_2$]·2H$_2$O[15] were prepared according to reported procedures. The ligands 2-phenyl-1,10-phenanthroline, 1,4-bis(2-[1,10]-phenanthrolinyl)benzene, and 4,4′-bis(2-[1,10]-phenanthrolinyl)biphenyl were prepared in earlier work.[3a]

3,2′-Dimethylene-2-phenyl-1,10-phenanthroline (3b). To a solution of 1-tetralone (**2b**, 248 mg, 1.70 mmol) and 8-amino-7-quinolinecarbaldehyde (**1**, 300 mg, 1.74 mmol) in absolute EtOH (25 mL) was added saturated ethanolic KOH (2 mL). The solution was refluxed under Ar for 78 h. After evaporation of solvent, the residue was redissolved in CH_2Cl_2 (30 mL) and then washed with H_2O (50 mL) to remove excess KOH. Concentration under reduced pressure, followed by column chromatography on alumina (40 g), eluting with hexanes/EtOAc (1:9), gave 340 mg of a burgundy oil which, when triturated with Et_2O (10 mL), provided **3b** (300 mg, 63%) as a beige solid, mp 145−147 °C: ^{1}H NMR (CD_3CN) δ 9.10 (dd, 1H, J = 3.0 Hz, H_9), 8.64 (dd, 1H, J = 6.0 Hz, $H_{6'}$), 8.34 (dd, 1H, J = 8.0 Hz, H_7), 8.12 (s, 1H, H_4), 7.81 (broad s, 2H, H_5/H_6), 7.66 (quartet, 1H, J = 3.5 Hz, H_8), 7.46 (t, 1H, J = 7.4 Hz, $H_{5'}$), 7.40 (t, 1H, J = 7.3 Hz, $H_{4'}$), 7.33 (d, 1H, J = 6.0 Hz, $H_{3'}$), 3.16 (t, 2H, H_α), 3.03 (t, 2H, $H_{\alpha'}$); ^{13}C NMR δ 153.5, 150.2, 150.1, 146.3, 145.0, 139.0, 136.4, 134.8, 134.5, 132.7, 129.8, 128.7, 128.3, 127.8, 127.5, 127.3, 126.0, 122.6, 28.8, 28.3. Anal. Calcd for $C_{20}H_{14}N_2$·1.75H$_2$O: C, 81.22; H, 5.24; N, 9.48. Found: C, 81.13; H, 4.59; N, 9.55.

3,2′-Trimethylene-2-phenyl-1,10-phenanthroline (3c). Following the procedure for **3b**, 1-benzosuberone (**2c**, 100 mg, 0.58 mmol) was condensed with **1** (93 mg, 0.6 mmol) in absolute EtOH to provide **3c** (90 mg, 52%) as a burgundy solid, mp 212−213 °C: ^{1}H NMR (CD_3CN) δ 9.09 (dd, 1H, J = 2.6 Hz, H_9), 8.36 (dd, 1H, J = 6.3 Hz, H_7), 8.19 (s, 1H, H_4), 7.88 (AB quartet, 2H, J = 3.0, 6.0 Hz, H_5/H_6), 7.85 (dd, 1H, J = 6.0 Hz, $H_{6'}$), 7.67 (quartet, 1H, J = 3.7 Hz, H_8), 7.46 (m, 2H, $H_{4'}$/$H_{5'}$), 7.35 (d, 2H, J = 6.0 Hz, $H_{3'}$), 2.71 (t, 2H, J = 6.0 Hz, H_α), 2.58 (t, 2H, J = 6.0 Hz, H_β), 2.28 (m, 2H, $H_{\alpha'}$); ^{13}C NMR δ 160.2, 150.2, 146.4, 144.8, 140.5, 139.2, 136.4, 135.5, 135.2, 130.2, 129.0, 128.5, 128.2, 128.0, 127.0, 126.4, 126.2, 122.5, 32.4, 31.0, 30.7. Anal. Calcd for $C_{21}H_{16}N_2$·1.00H$_2$O: C, 80.25; H, 5.73; N, 8.92. Found: C, 80.53; H, 4.58; N, 9.15.

Naphtho[1,2-*b*]-1,10-phenanthroline (3d). To a solution of 3,2′-dimethylene-2-phenyl-1,10-phenanthroline (**3b**, 220 mg, 0.78 mmol) in nitrobenzene (5 g) was added Pd/C (100 mg, 10%). The suspension was refluxed under Ar for 24 h, at which time a second portion of Pd/C (25 mg, 10%) and nitrobenzene (1 g) were added. Reflux was continued for another 24 h. The hot solution was filtered through Celite, and the Celite was rinsed with CH_2Cl_2 (3 × 10 mL). Concentration of the filtrate gave a thick liquid which was chromatographed on alumina (20 g) eluting first with CH_2Cl_2/hexanes (1:1) to provide unreacted **3b** and then with $CHCl_3$ to obtain an oily solid. This solid was washed with Et_2O/hexanes (1:1) to give **3d** (100 mg, 46%) as a beige solid, mp 198−200 °C: ^{1}H NMR (CD_3CN) δ 9.63 (d, 1H, J = 9.0 Hz, $H_{8'}$), 9.20 (dd, 1H, J = 3.0 Hz, H_9), 8.90 (s, 1H, H_4), 8.40 (dd, 1H, J = 9.0 Hz, H_7), 8.07−7.82 (m, 7H), 7.76 (m, 1H, H_8); ^{13}C NMR ($CDCl_3$) δ 149.9, 149.8, 147.4, 146.2, 137.0, 135.4, 135.3, 134.0, 129.3, 129.1, 127.9, 127.7, 127.5, 127.4, 126.8, 126.7, 126.4, 126.0, 125.3, 123.4. Anal. Calcd for $C_{20}H_{12}N_2$: C, 85.71; H, 4.28; N, 10.00. Found: C, 85.65; H, 4.11; N, 9.87.

3-Phenyl-1,10-phenanthroline (4). A mixture of 8-amino-7-quinolinecarbaldehyde (**1**, 258 mg, 1.5 mmol), phenylacetaldehyde (540 mg, 4.5 mmol), and piperidine (0.5 mL) in absolute ethanol (20 mL) was refluxed under Ar for 20 h. After cooling, H_2O (100 mL) was added and the reaction mixture was extracted with CH_2Cl_2 (2 × 50 mL). The CH_2Cl_2 layer was dried over anhydrous $MgSO_4$. The solvent was evaporated, and the residue was purified by column chromatography on alumina (20 g), eluting with methanol, to afford **4** as a brown solid (80 mg, 21%), mp 87−90 °C: ^{1}H NMR ($CDCl_3$) δ 9.44 (d, 1H, J = 1.8 Hz, H_2), 9.22 (d, 1H, J = 3.9 Hz, H_9), 8.41 (d, 1H, J = 2.1 Hz, H_4), 8.29 (d, 1H, J = 8.4 Hz, H_7), 7.85 (AB quartet, 2H, H_5 and H_6), 7.78 (d, 2H, J = 7.5 Hz, *o*-Ar), 7.66 (q, 1H, H_8), 7.56 (t, 2H, J = 7.2 Hz, *m*-Ar), 7.47 (t, 1H, J = 7.4 Hz, *p*-Ar); ^{13}C NMR ($CDCl_3$) δ 150.4, 149.4, 146.1, 145.1, 137.5, 136.0, 135.8, 133.4, 129.2, 128.6, 128.5, 128.4, 127.5, 126.9, 126.7.

Preparation of Ru(II) Complexes. [Ru(phen)(bpy-d_8)$_2$](PF$_6$)$_2$. A mixture of *cis*-[Ru(bpy-d_8)$_2$Cl$_2$]·2H$_2$O (151 mg, 0.3 mmol) and 1,10-phenanthroline (54 mg, 0.3 mmol) in ethanol/H_2O (3:1, 15 mL) was refluxed under Ar for 24 h under Ar. After cooling, a solution of NH_4PF_6 (98 mg, 0.6 mmol) in ethanol/H_2O (1:1, 5 mL) was added, and the mixture was stirred for 1 h at room temperature. The solvent was evaporated, and the residue was purified by chromatography on alumina (20 g), eluting with toluene/CH_3CN (1:2), to afford a red solid (135 mg, 50%): ^{1}H NMR (CD_3CN) δ 8.60 (d, 2H, J = 8.1 Hz, H_4 and H_7), 8.23 (s, 2H, H_5 and H_6), 8.07 (d, 2H, J = 4.2 Hz, H_2 and H_9), 7.72 (q, 2H, H_3 and H_8); MS *m*/*z* 304 (M).

[Ru(3a)(bpy-d_8)$_2$](PF$_6$)$_2$. Following the procedure described for [Ru(phen)(bpy-d_8)$_2$](PF$_6$)$_2$, a mixture of *cis*-[Ru(bpy-d_8)$_2$Cl$_2$]·2H$_2$O (80 mg, 0.15 mmol) and 2-phenyl-1,10-phenanthroline (**3a**, 38 mg, 0.15 mmol) in ethanol/H_2O (3:1, 20 mL) was refluxed for 20 h to provide a red solid (125 mg, 86%): ^{1}H NMR (CD_3CN) δ 8.69 (d, 1H, J = 8.1 Hz, H_4), 8.62 (d, 1H, J = 8.1 Hz, H_7), 8.31 (AB quartet, 2H, H_5 and H_6), 7.90 (d, 1H, J = 4.8 Hz, H_9), 7.66 (d, 1H, J = 8.1 Hz, H_3), 7.65 (t, 1H, J = 8.1 Hz, H_8), 7.32 (d, 1H, J = 6.6 Hz, $H_{2'}$), 7.05 (t, 1H, J = 6.9 Hz, $H_{3'}$), 7.00 (m, 1H, $H_{4'}$), 6.73 (t, 1H, J = 6.9 Hz, $H_{5'}$), 6.10 (d, 1H, J = 6.9 Hz, $H_{6'}$); MS *m*/*z* 342 (M).

[Ru((3b)bpy-d_8)$_2$](PF$_6$)$_2$. Following the procedure described for [Ru(phen)(bpy-d_8)$_2$](PF$_6$)$_2$, a mixture of *cis*-[Ru(bpy-d_8)$_2$Cl$_2$]·2H$_2$O (97 mg, 0.18 mmol) and 2-phenyl-3,2′-dimethylene-1,10-phenanthroline (**3b**, 51 mg, 0.18 mmol) in ethanol/H_2O (3:1, 20 mL) was refluxed for 24 h to provide a red solid (90 mg, 50%): ^{1}H NMR (CD_3CN, at −40 °C) δ 8.61 (d, 1H, J = 8.1 Hz, H_7), 8.33 (s, 1H, H_4), 8.16 (AB quartet, 2H, H_5 and H_6), 7.83 (d, 1H, J = 4.8 Hz, H_9), 7.69 (d, 1H, J = 7.5 Hz, $H_{6'}$), 7.56 (q, 1H, H_8), 7.01 (d, 1H, J = 7.5 Hz, $H_{3'}$), 6.94 (t, 1H, J = 7.2 Hz, $H_{4'}$), 6.80 (t, 1H, J = 7.2 Hz, $H_{5'}$), 2.90 (d, 2H, CH_2), 2.71 (d, 2H, CH_2); MS *m*/*z* 354 (M − 1).

[Ru(3c)(bpy-d_8)$_2$](PF$_6$)$_2$. Following the procedure described for [Ru(phen)(bpy-d_8)$_2$](PF$_6$)$_2$, a mixture of *cis*-[Ru(bpy-d_8)$_2$Cl$_2$]·2H$_2$O (107 mg, 0.20 mmol) and 2-phenyl-3,2′-trimethylene-1,10-phenanthroline (**3c**, 59 mg, 0.20 mmol) in ethanol/H_2O (3:1, 20 mL) was refluxed for 24 h to provide an orange red solid (115 mg, 57%): ^{1}H NMR (CD_3CN) (two sets of peaks representing two diastereomers in an approximate 4:3 ratio) δ 8.61 and 8.57 (two d, 1H, H_7), 8.55 and 8.42 (two s, 1H, H_4), 8.28−8.18 (two overlapping AB quartets, 2H, H_5 and H_6), 8.06 and 7.84 (two d, 1H, H_9), 7.64 and 7.59 (two d of d, 1H, H_8), 7.20 (d, 0.6H), 6.98−6.78 (overlapping m, 2.6H), 6.47 (t, 0.4H), 5.46 (d, 0.4H), 3.00−1.60 (overlapping m, 6 H); MS *m*/*z* 361 (M − 1).

[Ru(3d)(bpy-d_8)$_2$](PF$_6$)$_2$. A mixture of *cis*-[Ru(bpy-d_8)$_2$Cl$_2$]-2H$_2$O (84 mg, 0.16 mmol) and naphtho[1,2-*b*]-1,10-phenanthroline (**3d**, 44 mg, 0.16 mmol) in ethylene glycol (25 mL) was heated in microwave oven (70 W) under Ar for 25 min. After cooling, a solution of NH_4PF_6 (98 mg, 0.6 mmol) in H_2O (5 mL) was added and stirred at room temperature for 1 h. Water (5 mL) was added to the reaction mixture, and a precipitate was collected by filtration. The precipitate was purified by column chromatography on alumina (20 g), eluting with CH_3CN/toluene (1:2), to afford a red solid (59 mg, 37%): ^{1}H NMR (CD_3CN) δ 9.14 (d, 1H, J = 7.8 Hz, $H_{6'}$), 8.96 (s, 1H, H_4), 8.69 (d, 1H, J = 7.8 Hz, H_7), 8.24 (AB quartet, 2H, H_5 and H_6), 7.94 (d, 1H, J = 5.1 Hz, H_9), 7.82 (d, 1H, J = 9.0 Hz, ═CH), 7.73 (t, 1H, J = 7.8 Hz, $H_{3'}$), 7.69 (d, 1H, J = 9.0 Hz, ═CH), 7.68 (q, 1H, H_8), 7.41 (t, 1H, J = 7.2 Hz, $H_{4'}$), 7.16 (t, 1H, J = 7.5 Hz, $H_{5'}$); MS *m*/*z* 353 (M − 1).

[Ru(4)(bpy-d_8)$_2$](PF$_6$)$_2$. Following the procedure described for [Ru(phen)(bpy-d_8)$_2$](PF$_6$)$_2$, a mixture of *cis*-[Ru(bpy-d_8)$_2$Cl$_2$]·2H$_2$O (80 mg, 0.15 mmol) and 3-phenyl-1,10-phenanthroline (**4**, 38 mg, 0.15 mmol) in ethanol/H_2O (3:1, 15 mL) was refluxed for 36 h to provide a red solid (60 mg, 41%): ^{1}H NMR (CD_3CN) δ 8.83 (d, 1H, J = 1.8 Hz, H_4), 8.62 (d, 1H, J = 8.1 Hz, H_7), 8.26 (AB quartet, 2H, H_5 and H_6), 8.15 (d, 1H, J = 1.5 Hz, H_2), 8.08 (d, 1H, J = 5.1 Hz, H_9), 7.73 (q, 1H, H_8), 7.58−7.47 (m, overlapping, 5H, Ar); MS *m*/*z* 341 (M − 1).

[Ru(5)(bpy-d_8)$_2$](PF$_6$)$_2$. Following the procedure described for [Ru(bpy-d_8)$_2$(**3d**)](PF$_6$)$_2$, a mixture of 2,9-diphenyl-1,10-phenanthroline (**5**, 46 mg, 0.14 mmol) and *cis*-[Ru(bpy-d_8)$_2$Cl$_2$]·2H$_2$O (74 mg, 0.14 mmol) in ethylene glycol (25 mL) was heated in microwave oven (70 W) under Ar for 30 min to provide a brown red solid (67 mg, 46%): ^{1}H NMR (CD$_3$CN) δ 8.65 (d, 2H, J = 8.1 Hz, H$_4$ and H$_7$), 8.33 (s, 2H, H$_5$ and H$_6$), 7.53 (d, 2H, J = 8.1 Hz, H$_3$ and H$_8$), 7.12 (b, 2H, Ar), 7.01 (t, 2H, Ar), 6.85 (b, 2H, Ar), 6.72 (b, 2H, Ar), 6.11 (b, 2H, Ar); MS m/z 379 (M − 1).

[Ru(bpy-d_8)$_2$(6)Ru(bpy-d_8)$_2$](PF$_6$)$_4$. Following the procedure described for [Ru(phen)(bpy-d_8)$_2$](PF$_6$)$_2$, a mixture of **6** (10 mg, 0.023 mmol) and *cis*-[Ru(bpy-d_8)$_2$Cl$_2$]-2H$_2$O (25 mg, 0.047 mmol) in EtOH/H$_2$O (1:1, 4 mL) provided the complex as an orange-red solid (43 mg, 99%): ^{1}H NMR (600 MHz, CD$_3$CN) (two sets of peak in a 3:2 ratio for the two diastereomers), the major isomer δ 8.81 (d, J = 8.3 Hz, H$_{4'}$), 8.63 (dd, J = 8.3, 1.2 Hz, H$_{7'}$), 8.36 (d, J = 8.9 Hz, H$_{5'}$ or H$_{6'}$), 8.30 (d, J = 8.9 Hz, H$_{5'}$ or H$_{6'}$), 7.89 (dd, J = 5.2, 1.2 Hz, H$_{9'}$), 7.65 (dd, J = 8.2, 5.2 Hz, H$_{8'}$), 7.38 (d, J = 8.3 Hz, H$_{3'}$), 6.79 (dd, J = 7.8, 1.9 Hz, H$_2$, H$_5$), 5.89 (dd, J = 7.8, 1.9 Hz, H$_3$, H$_6$), the minor isomer δ 8.83 (d, J = 8.3 Hz, H$_{4'}$), 8.61 (dd, J = 8.3, 1.2 Hz, H$_{7'}$), 8.38 (d, J = 8.9 Hz, H$_{5'}$ or H$_{6'}$), 8.31 (d, J = 8.9 Hz, H$_{5'}$ or H$_{6'}$), 7.87 (dd, J = 5.2, 1.2 Hz, H$_{9'}$), 7.66 (dd, J = 8.2, 5.2 Hz, H$_{8'}$), 7.42 (d, J = 8.3 Hz, H$_{3'}$), 7.11 (s, H$_2$, H$_5$), 5.32 (s, H$_3$, H$_6$).

[Ru(bpy-d_8)$_2$(7)Ru(bpy-d_8)$_2$](PF$_6$)$_4$. Following the procedure described for [Ru(phen)(bpy-d_8)$_2$](PF$_6$)$_2$, a mixture of *cis*-[Ru(bpy-d_8)$_2$-Cl$_2$]·2H$_2$O (54 mg, 0.1 mmol) and 4,4′-bis(2-[1,10]-phenanthrolinyl)-biphenyl (20 mg, 0.04 mol) in ethanol/H$_2$O (3:1, 20 mL) was refluxed for 20 h to provide a dark red solid (32 mg, 41%): ^{1}H NMR (CD$_3$CN) δ 8.75 (d, 2H, J = 8.4 Hz, H$_4$), 8.64 (d, 2H, J = 7.8 Hz, H$_7$), 8.34 (AB quartet, 4H, H$_5$ and H$_6$), 7.90 (d, 2H, J = 4.8 Hz, H$_9$), 7.72 (d, 2H, J = 8.1 Hz, H$_3$), 7.66 (t, 2H, J = 8.1 Hz, H$_8$), 7.40 (b, 2H), 7.12 (b, 2H), 6.79 (b, 2H), 6.22 (b, 2H); MS m/z 341 (M − 1).

X-ray Determination of [(bpy)$_2$Ru(6)Ru(bpy)$_2$](PF$_6$)$_4$. A dark orange-red wedge having approximate dimensions 0.50 × 0.20 × 0.15 mm was mounted in a random orientation on a Nicolet R3m/V automatic diffractometer. Since the crystals were known to decompose rapidly outside of the mother liquor, the sample was placed in a stream of dry nitrogen gas at −50 °C. The radiation used was Mo Kα monochromatized by a highly ordered graphite crystal. Final cell constants, as well as other information pertinent to data collection and refinement, are listed in Table 7. The Laue symmetry was determined to be $\bar{1}$, and the space group was shown to be either $P1$ or $P\bar{1}$. Intensities were measured using the θ:2θ scan technique, with the scan rate depending on the count obtained in rapid prescans of each reflection. Two standard reflections were monitored after every 2 h or every 100 data collected, and these showed no significant change over the course of the experiment. During data reduction Lorentz and polarization corrections were applied; however, no correction for absorption was made due to the small absorption coefficient.

The unitary structure factors displayed centric statistics, and so space group $P\bar{1}$ was assumed from the outset. The structure was solved by interpretation of the Patterson map, which revealed the position of the Ru atom in the asymmetric unit, consisting of one-half cation situated about an inversion center, two anions, and two molecules of acetone solvent. Remaining non-hydrogen atoms were located in subsequent difference Fourier syntheses. The usual sequence of isotropic and anisotropic refinement was followed, after which all hydrogens were entered in ideal calculated positions and constrained to riding motion, with a single variable isotropic temperature factor for all of them. No attempt was made to include hydrogens on the acetone solvent molecules. After all shift/esd ratios were less than 0.1 convergence was reached at the agreement factors listed in Table 1. No unusually high correlations were noted between any of the variables in the last cycle of full-matrix least squares refinement, and the final difference density map showed a maximum peak of about 0.8 e/A^3. All calculations were made using Nicolet's SHELXTL PLUS (1987) series of crystallographic programs.[22]

Table 7. Data Collection and Processing Parameters for [(bpy)$_2$Ru(**6**)Ru(bpy)$_2$](PF$_6$)$_4$

space group	$P\bar{1}$ (triclinic)
cell constants	a = 12.427(5) Å
	b = 13.655(5) Å
	c = 14.500(5) Å
	α = 65.60(2)°
	β = 75.01(3)°
	γ = 85.33 (3)°
	V = 2164 Å^3
mol formula	$C_{70}H_{50}N_{12}Ru_2^{4+}(PF_6^-)_4$·4$C_3H_6O$
fw	2073.70
formula units per cell	Z = 1
density	ρ = 1.59 g cm^{-3}
abs coeff	μ = 5.20 cm^{-1}
temp	T = −50 °C
radiation (Mo Kα)	λ = 0.710 73 Å
R^a	0.042
$R_w{}^b$	0.041
weights	$w = \sigma(F)^{-2}$

^{a} $R = \sum||F_o| - |F_c||/\sum |F_o|$. ^{b} $R_w = [\sum w(|F_o| - |F_c|)^2/\sum w|F_o|^2]^{1/2}$.

Acknowledgment. R.P.T. thanks the Robert A. Welch Foundation, the National Science Foundation (Grant CHE-9714998), and the Petroleum Research Fund of the American Chemical Society. R.H.S. thanks the Division of Chemical Sciences, Office of Basic Energy Sciences, U.S. Department of Energy (Contract No. DE-FG02-96ER14617) for support of this work. We also thank Drs. Chi-Ying Hung and Matthias Pohl for assistance with ligand **6** and its complex, Dr. James Korp for assistance with the X-ray determination, and Prof. Debbie Roberts for assistance with the mass spectroscopy.

Supporting Information Available: Figure S1, showing the numbering scheme for the X-ray determination of [(bpy)$_2$Ru(**6**)Ru(bpy)$_2$](PF$_6$)$_4$, and Figure S2, showing the crystal packing diagram, as well as tables of atomic coordinates, bond lengths, bond angles, anisotropic displacement parameters, and H atom coordinates. This material is available free of charge via the Internet at http://pubs.acs.org.

IC990706Y

(19) Simon, J. A.; Curry, S. L.; Schmehl, R. H.; Schatz, T. R.; Piotrowiak, P.; Jin, X.; Thummel, R. P. *J. Am. Chem. Soc.* **1997**, *119*, 11012.
(20) Goulle, V.; Thummel, R. P. *Inorg. Chem.* **1990**, *29*, 1767.
(21) Chirayil, S.; Thummel, R. P. *Inorg. Chem.* **1989**, *28*, 813.
(22) Sheldrick, G. M. In *Crystallographic Computing 3;* Sheldrick, G. M., Kruger, C., Goddard, R., Eds.; Oxford University Press: Oxford, U.K., 1985; pp 175−189.